# Gadolinium Nitride Gd3N in Carbon Cages: The Influence of Cluster Size and Bond Strength

cluster fullerenes with larger RE trimetal nitrides. Moreover it has to be addressed whether higher fullerene cages than $C_{80}$ could be stabilized by larger RE trimetal nitrides. Therefore it is interesting whether $Gd_3N$ cluster fullerenes can be prepared and isolated at all. From the point of medical applications, $Gd_3N$ cluster fullerenes might yet be the precursor compounds of choice for nontoxic MRI agents with unprecedented relaxivities.

Herein the preparation of $Gd_3N@C_{2n}$ $(40 \leq n \leq 44)$ cluster fullerenes and the isolation of the $Gd_3N@C_{80}(I)$ isomer is reported. Its chemical identity and purity were established by mass spectrometry and high-pressure liquid chromatography (HPLC). The optical energy gap and the electronic absorptions were determined by Vis-NIR spectroscopy. Magnetic properties of $Gd_3N@C_{80}(I)$ were probed by EPR spectroscopy. The cage isomer of the $Gd_3N@C_{80}(I)$ was verified using Vis-NIR and FTIR spectroscopy. Raman spectroscopy was used to analyze the bonding between the caged $Gd_3N$ cluster and the $C_{80}$ cage. The analysis revealed two important factors that influence the abundance and stability of nitride-cluster fullerenes.

The chromatogram (Figure 1 a) and the mass spectroscopic analysis of the fullerene extract, give evidence for the formation of $Gd_3N$ cluster fullerenes with cages as small as $C_{80}$ and as large as $C_{88}$. $Gd_3N@C_{80}$ is the most abundant fullerene in the extract. Its relative yield is approximately 35–40% of all fullerenes formed, which is by a factor of about two smaller than the relative yields of $Sc_3N@C_{80}$ and $Tm_3N@C_{80}$.[15, 16] The

## Endohedral Fullerenes

# Gadolinium Nitride Gd₃N in Carbon Cages: The Influence of Cluster Size and Bond Strength**

*Matthias Krause\* and Lothar Dunsch*

Endohedral fullerenes have intriguing structural, magnetic, and electronic properties which may hold vast potential for applications in electronics and medicine.[1,2] Among possible applications, their use as contrast agents in magnetic resonance imaging (MRI) is currently intensively discussed.[3–6] Recently up to 20 times higher proton relaxivities were reported for $Gd@C_{82}(OH)_n$ fullerenols in comparison to $Gd^{3+}$ chelate contrast agents.[4,5] Increased magnetic dipole–dipole relaxation was made responsible for this behavior. Hence, even higher proton relaxivities can be expected for endohedral fullerenes with two or three encaged metal ions, provided that their magnetic moments are coupled ferromagnetic. The spatial shielding of the $Gd^{3+}$ ions by the carbon cage prevents their accumulation in human organs and tissues. Owing to this unique combination of crucial properties endohedral gadolinium fullerenes could replace current MRI agents in the future.

The discovery of $Sc_3N@C_{80}$ in 1999 opened the gate to fullerene structures with an encaged trimetal nitride cluster.[7] The $C_{80}:7(I_h)$[8] cage isomer was recognized as the most abundant fullerene cage for different trimetal nitrides, such as $Sc_3N$, $Y_3N$, and $RE_3N$ (RE = rare-earth metals Tb, Ho, Er, Tm, Lu).[9–14, 16] No attempts to include larger nitride clusters than $Tb_3N$ into carbon cages have been reported up to date. It is an open question, whether a stability threshold exists for $C_{80}$

[*] Dr. M. Krause, Prof. Dr. L. Dunsch
Leibniz-Institute for Solid State and Materials Research Dresden
Institute of Solid State Research
Group for Electrochemistry and Conducting Polymers
Postfach 27 01 16, 01171 Dresden (Germany)
Fax: (+49) 351-465-9745
E-mail: m.krause@ifw-dresden.de

***Figure 1.*** a) Chromatogram of the $Gd_3N$–fullerene extract and separation limits for $Gd_3N@C_{80}$ (I), $1 = Gd_3N@C_{80}$, $2 = Gd_3N@C_{82}$, $3 = Gd_3N@C_{86}$, $4 = Gd_3N@C_{84}$, $5 = Gd_3N@C_{88}$, flow rate 1.6 mL min⁻¹, injection volume 100 μL, 30°C; the background at low retention times is due to hydrocarbon byproducts. b) Chromatogram of isolated $Gd_3N@C_{80}$ (I), conditions as for (a). c) Positive ion LD-TOF mass spectrum of isolated $Gd_3N@C_{80}$ (I).

$Gd_3N@C_{80}$ HPLC fraction was composed of the $Gd_3N@C_{80}$ (I) isomer, whose retention time is 39.6 min, and the $Gd_3N@C_{80}$ (II) minor isomer giving rise to a small peak at $t = 41.5$ min. These retention times agree with those of $Sc_3N@C_{80}$ (I, II) and $Tm_3N@C_{80}$ (I, II) within a time interval of $\pm 1$ min.[15,16] The relative abundance of the second isomer in the entire $Gd_3N@C_{80}$ fraction was approximately 10% and hence only half as high as for $Sc_3N@C_{80}$ (II) and $Tm_3N@C_{80}$ (II).[15,16] The fractions at retention times higher than 45 min were assigned to $Gd_3N$-cluster fullerenes with cages larger than $C_{80}$: $Gd_3N@C_{82}$, $Gd_3N@C_{86}$, $Gd_3N@C_{84}$, and $Gd_3N@C_{88}$. Their relative abundance was higher than within the $Tm_3N@C_{2n}$ ($39 \leq n \leq 43$) cluster fullerene family, in which nitride-cluster fullerenes beyond $C_{80}$ were observed for the first time.[16] On the other hand no $Gd_3N$ in cages smaller than $C_{80}$ was detected, in contrast to the examples of $Sc_3N@C_{68}$,[17] $Sc_3N@C_{78}$,[18] $Tm_3N@C_{76}$,[16] and $Tm_3N@C_{78}$.[16] $Gd_3N$ is the largest $RE_3N$ cluster caged in a fullerene to date. Assuming a trigonal-planar structure and taking into account the expression $d(RE_3N) \propto 4r(RE^{3+})$ for the cluster diameter $d$, the $Gd_3N$ cluster is by approximately 0.8 Å larger than $Sc_3N$ ($r(Gd^{3+}) = 0.94$ Å, $r(Sc^{3+}) = 0.75$ Å).[19] Apparently $C_{80}$ represents the size threshold for the encapsulation of the $Gd_3N$ cluster in fullerene cages.

In the following we focus on the electronic and geometric properties of $Gd_3N@C_{80}$ (I), the most abundant $Gd_3N$ structure. Its chemical identity and the purity of $> 95\%$ are shown by the chromatogram and the mass spectrum in Figure 1. Its successful isolation shows that the $C_{80}$ cage is large enough to form a stable $Gd_3N@C_{80}$ (I) cluster fullerene. The lower relative abundance of $Gd_3N@C_{80}$ (I) in comparison to $Sc_3N@C_{80}$ (I) and $Tm_3N@C_{80}$ (I) poses the question of whether this is due to a smaller energy gap, a different cage structure, or different bonding properties of the nitride clusters?

The Vis-NIR spectrum in Figure 2a reveals a large energy-gap electronic structure of $Gd_3N@C_{80}$ (I). The spectral onset is at around 780 nm. The HOMO–LUMO transition has a doublet structure with absorption maxima at 706 and 676 nm. The strongest visible absorption of $Gd_3N@C_{80}$ (I) is at 412 nm, and a shoulder is apparent at 555 nm. For comparison, $Tm_3N@C_{80}$ (I) has an onset at 780 nm, the HOMO–LUMO transitions at 705 and 675 nm, and the strongest absorptions at 540 and 407 nm.[16] The electronic absorption spectra of $Gd_3N@C_{80}$ (I) and $Tm_3N@C_{80}$ (I) agree almost completely. Hence, neither a smaller energy gap nor the electronic structure of the $C_{80}$ cage can be responsible for the lower abundance of $Gd_3N@C_{80}$ (I) in comparison to $Sc_3N@C_{80}$ (I) and $Tm_3N@C_{80}$ (I).

Electron spin resonance of $Gd_3N@C_{80}$ (I) powder was studied by X-band continuous wave (cw) EPR spectroscopy at 4 and 295 K. No EPR signal for the fullerene was detected in these experiments. This result shows a diamagnetic electronic state for the $C_{80}$ carbon cage in $Gd_3N@C_{80}$ (I), similar to the cases of $Sc_3N@C_{80}$ (I) and $Tm_3N@C_{80}$ (I). On the other hand, an EPR signal from the $(4f)^7$ states of the endohedral $Gd^{3+}$ ions is expected. The $g$ factor would be 2 and a resonance should appear at a magnetic induction of around 340 mT. The absence of this signal might be due to a strong line broadening in the powder sample. This problem can be
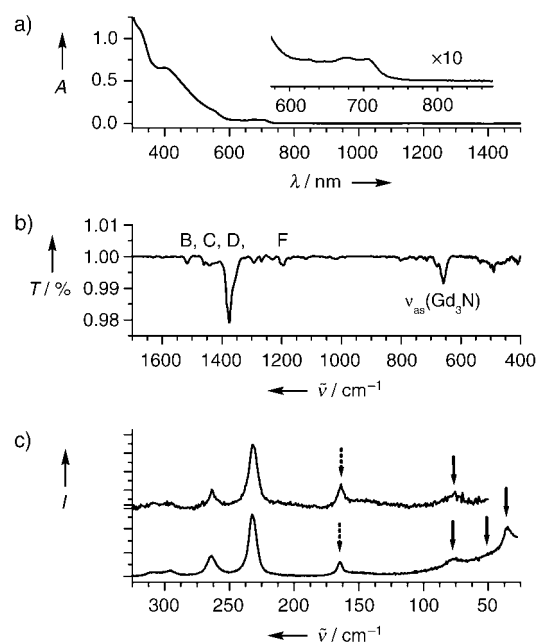


**Figure 2.** a) Vis-NIR spectrum of $Gd_3N@C_{80}$ (I) dissolved in toluene, 10-mm path length, 2 nm resolution. b) FTIR spectrum of $Gd_3N@C_{80}$ (I), 500 accumulations, 2 cm$^{-1}$ resolution, capitals refer to the line-group classification introduced in refs. [15, 16]. c) Low-energy Raman spectrum of $Gd_3N@C_{80}$ (I), excited with 514 nm (upper trace) and 647 nm (lower trace) laser radiation, solid arrows indicate $Gd_3N-C_{80}$ vibrations, the broken arrows mark an internal $Gd_3N$ cluster deformation mode.

overcome by future EPR studies in the W-band range, which have been successfully applied to detect the spin states in $Gd@C_{82}$.[20]

The FTIR spectrum of $Gd_3N@C_{80}$ (I) in Figure 2b shows a small number of lines. This situation is characteristic for a $C_{80}$ cage with high symmetry. The detailed analysis revealed the same tangential cage-mode line groups as observed for the icosahedral structures $Sc_3N@C_{80}$ (I) and $Tm_3N@C_{80}$ (I).[15,16] As for these compounds, only one strong radial cage mode was found at around 500 cm$^{-1}$ for $Gd_3N@C_{80}$ (I).[15,16] Owing to the close resemblance of its FTIR spectrum to those of $Sc_3N@C_{80}$ (I) and $Tm_3N@C_{80}$ (I), $Gd_3N@C_{80}$ (I) is assigned to the same carbon cage, that is, $C_{80}$:7 with $I_h$ symmetry (Figure 3). This assignment is strongly supported by the HPLC and Vis-NIR analysis.

There is one major difference between the IR spectra of $Gd_3N@C_{80}$ (I), $Tm_3N@C_{80}$ (I), and $Sc_3N@C_{80}$ (I). The most intense low-energy IR line is at approximately 710 cm$^{-1}$ for $Tm_3N@C_{80}$ (I), at 657 cm$^{-1}$ for $Gd_3N@C_{80}$ (I), and at 599 cm$^{-1}$ for $Sc_3N@C_{80}$ (I). Owing to its comparable intensity and the unambiguous metal-induced shift, this line is assigned to the antisymmetric M−N stretching vibration of the $M_3N$ (M = Tm, Gd, Sc) cluster. For an explanation of the lower formation abundance of $Gd_3N@C_{80}$ (I) the frequency downshift of 53 cm$^{-1}$ compared to $Tm_3N@C_{80}$ (I) is important. The lower vibrational energy reflects a weaker metal–nitrogen bond in $Gd_3N$. A mutual stabilization of the nitride cluster and the $C_{80}$:7($I_h$) carbon cage is responsible for the unusual high abundance and stability of these structures.[10,11] If one
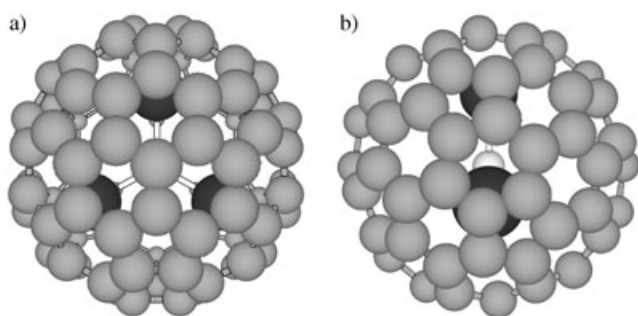
**Figure 3.** Schematic structure model of Gd$_3$N@C$_{80}$ (I$I_h$) in orientation a) along and b) perpendicular to the $C_3$ axis; black Gd, gray C, white N; the geometry and orientation of the Gd$_3$N cluster are still to be confirmed.

component becomes less stable, the whole cluster fullerene will be destabilized and/or the formation of the structure will be suppressed. Thus, the weaker metal–nitrogen bond in Gd$_3$N is an important quantity in explaining the smaller yield of Gd$_3$N@C$_{80}$(I). It can be rationalized by the weaker overlap of the Gd 5d and N 2p atomic orbitals, which is responsible for the chemical bond in the cluster. However, this bond-strength difference accounts only partly for the observed abundances, as the Sc$_3$N bond is even weaker than that of Gd$_3$N.

Another important factor for the overall stability of trimetal-nitride-cluster fullerenes is the interaction between the caged cluster and the carbon cage. As Figure 2c shows a typical vibrational pattern with low-energy Raman lines at 165, 77, 54, and 34 cm$^{-1}$ is evident for Gd$_3$N@C$_{80}$(I). The line at 165 cm$^{-1}$ has counterparts in the Raman spectra of Sc$_3$N@C$_{80}$ at 210 cm$^{-1}$[11] and at 194 cm$^{-1}$ for Y$_3$N@C$_{80}$[11] and is attributed to a Gd$_3$N cluster-deformation mode. The lines below 100 cm$^{-1}$ are assigned to frustrated Gd$_3$N rotations and translations. The frustration is due to Gd$_3$N–C$_{80}$ bond formation, which prevents a free cluster rotation as well as a cluster diffusion within the vibrational time scale of 10$^{-11}$–10$^{-13}$ s. For the alternative configurations of either a free-rotating cluster or a fast rotational diffusion, different low-energy Raman spectra are expected. For the free-rotating-cluster case, the rotation perpendicular to the cluster plane (R$_x$ and R$_y$) has $E''$ symmetry and is Raman allowed. Therefore a multiline rotational Raman spectrum is expected. For the fast rotational-diffusion case, the rotational Raman spectrum should be broadened into a continuous background without any resolved lines.

Plotting the frequencies of the low-energy Raman modes for several M$_3$N@C$_{80}$ (M = Sc, Y, Gd, Tb, Ho, Er, Tm) versus $(1/\mu(M_3N-C_{80}))^{1/2}$ a fairly good linear correlation is obtained. Therefore, to a good approximation, the bond force constants are the same. Thus, the same type and strength of cluster–cage interaction exists in all these nitride-cluster fullerene structures. Hence, a weaker cluster–C$_{80}$ interaction can be excluded as being significant for the lower abundance of Gd$_3$N@C$_{80}$(I).

Summarizing, endohedral Gd$_3$N-cluster fullerenes covering cage sizes from C$_{80}$ up to C$_{88}$ were prepared for the first time. Gd$_3$N@C$_{80}$(I) was the most abundantly formed fullerene structure in the soot, although larger Gd$_3$N-cluster fullerenes

were formed to a greater extend than within the Tm$_3$N@C$_{2n}$ ($39 \leq n \leq 43$) family. Gd$_3$N@C$_{80}$(I) is based on the C$_{80}$ cage isomer C$_{80}$:7 ($I_h$) and has a HOMO–LUMO energy gap of 1.75 eV. The Gd$_3$N cluster was found to form a bond to the C$_{80}$ cage. The Gd$_3$N is the largest cluster to be caged in fullerenes to date. Two factors influence the formation abundance and distribution of nitride-cluster fullerenes: the metal-ion radius and the metal–nitrogen bond strength.

## Experimental Section

The nitride-cluster fullerene preparation and isolation was described in detail elsewhere.[10,15,16] Briefly, ammonia gas (20 mbar) was added to the helium atmosphere in the Krätschmer–Huffman arc burning reactor. Mixtures of Gd$_2$O$_3$ powder and graphite powder were pressed into the holes of graphite-rod electrodes in a molar metal/carbon ratio of 1:12.5. The fullerene soot generated was purified with acetone and subsequently extracted by CS$_2$ for 20 h in a soxhlet extractor. On average 100 µg fullerenes were obtained per burning. Fullerene separation was by multistage HPLC with toluene as the eluent. Gd$_3$N@C$_{80}$(I) was isolated in one step using a linear combination of two analytical (4.6 × 250 mm) BuckyPrep columns (Nacalai Tesque). 250 µg Gd$_3$N@C$_{80}$(I) were isolated in this study. The composition of the extract and the purity of isolated Gd$_3$N@C$_{80}$(I) were determined by HPLC and laser desorption time-of-flight (LD-TOF) mass spectrometry. Sample preparation and experimental details for Vis-NIR, FTIR, and Raman measurements were described elsewhere.[15,16] Electron spin resonance (EPR) of Gd$_3$N@C$_{80}$(I) powder was measured using an EMX X-band spectrometer (Bruker) with 100 kHz modulation and a microwave power of 100 mW at room temperature, and 10 mW and 100 mW at 4 K. The sample was evacuated under high vacuum and sealed in a 4-mm diameter quartz tube.

[1] H. Shinohara, *Rep. Prog. Phys.* **2000**, *63*, 843–892.
[2] *Endofullerenes: A New Family of Carbon Clusters* (Eds.: T. Akasaka, S. Nagase), Kluwer Academic Publishers, Dordrecht, **2002**.
[3] L. J. Wilson, D. W. Cagle, T. P. Thrash, S. J. Kennel, S. Mirzadeh, J. M. Alford, G. J. Ehrhardt, *Coord. Chem. Rev.* **1999**, *192*, 199–207.
[4] M. Mikawa, H. Kato, M. Okumura, M. Narataki, Y. Kanazawa, N. Miwa, H. Shinohara, *Bioconjugate Chem.* **2001**, *12*, 510–514.
[5] H. Kato, Y. Kanazawa, M. Okumura, A. Taninaka, T. Yokawa, H. Shinohara, *J. Am. Chem. Soc.* **2003**, *125*, 4391–4397.
[6] R. D. Bolskar, A. F. Benedetto, L. O. Husebo, R. E. Price, E. F. Jackson, S. Wallace, L. J. Wilson, J. M. Alford, *J. Am. Chem. Soc.* **2003**, *125*, 5471–5478.
[7] S. Stevenson, G. Rice, T. Glass, K. Harich, F. Cromer, M. R. Jordan, J. Craft, E. Hajdu, R. Bible, M. M. Olmstead, K. Maitra, A. J. Fisher, A. L. Balch, H. C. Dorn, *Nature* **1999**, *401*, 55–57.
[8] P. W. Fowler, D. E. Manolopoulos, *An Atlas of Fullerenes*, Clarendon Press, Oxford, **1995**.
[9] L. Dunsch, P. Georgi, M. Krause, Ch. R. Wang, *Synth. Met.* **2003**, *135–136*, 761–762.
[10] L. Dunsch, M. Krause, J. Noack, P. Georgi, *J. Phys. Chem. Solids* **2004**, *65*, 309–315.

[11] M. Krause, H. Kuzmany, P. Georgi, L. Dunsch, K. Vietze, G. Seifert, *J. Chem. Phys.* **2001**, *115*, 6596–6605.

[12] L. Feng, J. X. Xu, Z. J. Shi, X. R. He, Z. N. Gu, *Chem. J. Chin. Univ.* **2002**, *23*, 996–998.

[13] E. B. Iezzi, J. C. Duchamp, K. R. Fletcher, T. E. Glass, H. C. Dorn, *Nano Lett.* **2002**, *2*, 1187–1190.

[14] M. M. Olmstead, A. de Bettencourt-Dias, J. C. Duchamp, S. Stevenson, H. C. Dorn, A. L. Balch, *J. Am. Chem. Soc.* **2000**, *122*, 12220–12226.

[15] M. Krause, L. Dunsch, *ChemPhysChem* **2004**, *5*, 1445–1449.

[16] M. Krause, J. Wong, L. Dunsch, *Chem. Eur. J.* **2005**, *11*, 706–711.

[17] S. Stevenson, P. W. Fowler, T. Heine, J. C. Duchamp, G. Rice, T. Glass, K. Harich, E. Hajdu, R. Bible, H. C. Dorn, *Nature* **2000**, *408*, 427–428.

[18] M. M. Olmstead, A. de Bettencourt-Dias, J. C. Duchamp, S. Stevenson, D. Marciu, H. C. Dorn, A. L. Balch, *Angew. Chem.* **2001**, *113*, 1263–1265; *Angew. Chem. Int. Ed.* **2001**, *40*, 1223–1225.

[19] N. N. Greenwood, A. Earnshaw, *Chemistry of the Elements*, Pergamon, Oxford, **1984**.

[20] "Electron spin resonance spectroscopy for metallofullerenes" in: T. Kato in *Endofullerenes*: *A New Family of Carbon Clusters* (Eds.: T. Akasaka, S. Nagase), Kluwer Academic Publishers, Dordrecht, **2002**, pp. 153–167.